Powder Technology 217 (2012) 7–10

Contents lists available at SciVerse ScienceDirect

Powder Technology

journal homepage: www.elsevier.com/locate/powtec

Thermoluminescence of combustion synthesized yttrium oxide

B.N. Lakshminarasappa [a,*], J.R. Jayaramaiah [a,b], B.M. Nagabhushana [c]

[a] *Department of Physics, Bangalore University, Bangalore-560 056, India*
[b] *Department of Physics, Government First Grade College, Hangal-581 104, India*
[c] *Department of Chemistry, M.S. Ramaiah Institute of Technology, Bangalore-560 054, India*

ARTICLE INFO

Article history:
Received 14 April 2011
Received in revised form 18 September 2011
Accepted 22 September 2011
Available online 1 October 2011

Keywords:
Nanoparticles
Combustion synthesis
Scanning electron microscopy
Oxides
Thermoluminescence

ABSTRACT

Pure yttrium oxide (Y_2O_3) was prepared by solution combustion technique using disodium ethylene diamine tetra acetic acid (EDTA-Na_2) as fuel at ~350 °C. Powder X-ray diffraction (PXRD) pattern of Y_2O_3 revealed cubic crystalline structure with crystallite size in the range of 18–23 nm. The scanning electron microscopy (SEM) indicated the foamy and fluffy nature of the sample. Fourier transformed infrared spectroscopy (FTIR) revealed four prominent absorption with peaks at 3395, 1433, 875 and 566 cm^{-1}. From the optical absorption studies the energy gap of the synthesized sample was found to be 5.72 eV. Two well resolved thermoluminescence (TL) glows with peaks at 475 and 626 K were observed in γ-irradiated Y_2O_3. The glow curves were analyzed and the average activation energy was found to be 0.505 and 0.977 eV respectively.

1. Introduction

Different techniques are applied to prepare nanocrystals. They include solid state reaction [1], wet chemical methods such as chemical vapor deposition [2], combustion [3,4], sol–gel [5], aerosol pyrolysis [6] etc. The solid state reaction method has several shortcomings such as prolonged reaction time, larger size grain growth and poor homogeneity. However, the salient features of wet chemical methods are that the starting materials can be mixed at molecular level and the temperature of formation of the final products is as low as that of conventional solid-state reactions techniques. Among wet chemical methods, 'solution combustion synthesis' has several advantages. It requires simple apparatus and the materials used are more economical [7,8]. It requires low energy, short time and this technique may also be employed to produce homogeneous, high-purity, crystalline oxides. The nature of crystallinity, surface area and agglomeration of the synthesized products are primarily governed by flame temperature during combustion which itself dependents on the nature of the fuel and the fuel-to-oxidizer ratio [9]. It is known that, a good fuel should react non-violently without producing toxic gasses and act as a complexing agent for metal ions [10]. EDTA-Na_2 is one such compound which serves as a fuel during the combustion reaction and gets oxidized by nitrate ions and this is used as a new technology for material synthesis [11]. This EDTA has several remarkable advantages in comparison with other fuels and it has the greater ability to chelate metal cations and forming very stable and soluble complexes. In this technique, the starting materials are mixed at the molecular or the atomic level in a solution and it is easy to control the composition and a high degree of homogeneity is obtained. It is an exothermic reaction and occurs with the evolution of heat and light. When the mixture of fuel and oxidizer is ignited, combustion takes place at high temperature and leads to growth of materials with nano crystalline form. Metal nitrates and hydrazine based compounds are used as oxidizer and fuels respectively to synthesize metal oxides [12].

Oxide phosphors are found to be suitable for field emission display (FED), vacuum fluorescent display (VFD), plasma panel display (PDP) and electroluminescence (EL) devices. Luminescence efficiency is found to increase as the size of the phosphor particle is decreased and the preparation of phosphor powders becomes very important in technological application [13]. When thermoluminescent material is exposed to γ-radiation, it absorbs and stores energy in the form of defects. A part of the stored energy is released in the form of visible light when the two types of defect centers are recombined upon warming the material.

Metal oxide matrix is proved to be an excellent host material for lasing action. The Y_2O_3 possesses high refractory properties, a high melting point (~2450 °C) and a high thermal conductivity (33 $Wm^{-1}\,K^{-1}$). It is a suitable material for photonic waveguide due to its high band gap (5.72 eV), with a very high refractive index (~2) and a wide transmission range (280–8000 nm) [14]. Numerous techniques are applied on the synthesis of rare earth doped nanocrystalline Y_2O_3 [15–18].

In the present work, Y_2O_3 nanopowder was synthesized by solution combustion technique in which EDTA-Na_2 was used as the chelating-fuel. Further, the TL behavior of the γ-irradiated Y_2O_3 has been studied and the enhancement in TL intensity with γ-ray dose was found. In

---

[*] Corresponding author. Tel.: +91 9448116281; fax: +91 80 23219295.
E-mail address: bnlnarasappa@rediffmail.com (B.N. Lakshminarasappa).

0032-5910/$ – see front matter © 2011 Elsevier B.V. All rights reserved.
doi:10.1016/j.powtec.2011.09.042

addition the material was found to be a potential candidate in TL dosimetry.

2. Experimental

The stoichiometry of the redox mixture used for combustion process was calculated using the total oxidizing and reducing valencies of the ingredients which serve as numerical co-efficients for the stoichiometric balance. The equivalence ratio, i.e. the ratio of the oxidizing valency to reducing valency was maintained at unity. According to the concept used in propellant chemistry, the valency of C is +4, H is +1, O is +2, divalent metal ions is +2, trivalent metal ions is +3 and so on. Based on these considerations, oxidizing valency of $Y(NO_3)_3$ is −15 and reducing valency of EDTA-Na_2 is +40. The valency of nitrogen was not considered.

The starting materials used for the 'solution combustion synthesis' of Y_2O_3 systems were yttrium oxide (99.99%, S.d.fine-chem), nitric acid and EDTA-Na_2. During synthesis, yttrium oxide was converted into yttrium nitrate by dissolving yttrium oxide in 1:1 nitric acid and excess nitric acid was removed by evaporation on a sand bath. The EDTA-Na_2 was dissolved in double distilled water and the solution was poured into a crystalline dish containing yttrium nitrate. The stoichiometric solution was stirred well to ensure a homogeneous solution. The solution was placed in a muffle furnace and maintained at ~350 °C. The reaction mixture underwent thermal dehydration and ignited at one spot with liberation of gaseous products such as oxides of nitrogen and carbon. The liberation of gaseous products during combustion reaction increases the surface area of the powder product, creating micro and nanoporous regions. The combustion propagated throughout the reaction mixture without further need of any external heating, as the heat of reaction is sufficient for the decomposition of the redox mixture. The process was completed in about five minutes and resulted in voluminous Y_2O_3 nano powder.

The synthesized material was characterized by the powder X-ray diffraction technique (Phillips X-ray Cu-K_α). The morphology of the synthesized sample was studied by scanning electron microscopy (JEOL JSM-840A). The Fourier-transformed infrared absorption spectra were recorded using Nicollet Magna 550 spectrometer with KBr pellets in the range of 400–4000 cm^{-1}. The energy gap of the material was calculated using ELICO (SL-159) UV–VIS spectrophotometer. The TL glow curves of γ-irradiated (^{60}Co) Y_2O_3 samples were obtained in the temperature range of 350 to 650 K, using a homemade TL set up consisting of a thin metallic heating strip, temperature programmer, photomultiplier tube (RCA 931A) and a multimeter (Rishicom) at a heating rate of 5 °C s^{-1}. The TL glow curves were deconvoluted using Origin software and TL parameters were calculated.

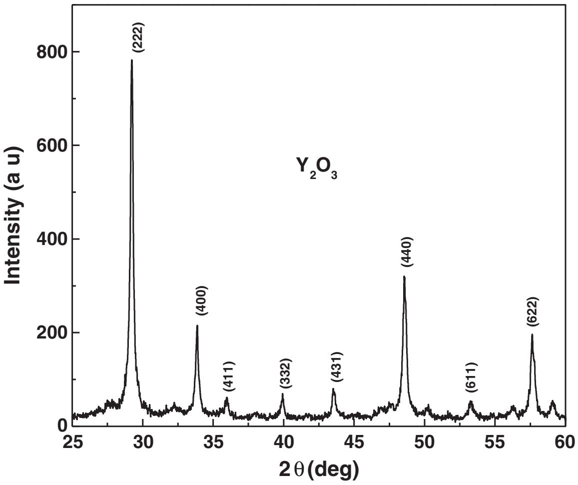

Fig. 1. PXRD spectrum of combustion synthesized Y_2O_3.

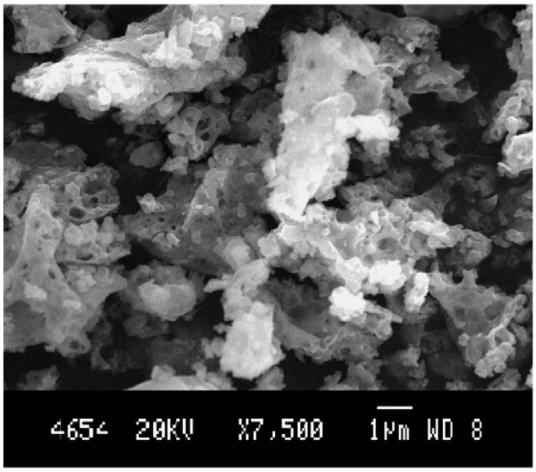

Fig. 2. SEM photograph of combustion synthesized Y_2O_3.

3. Results and discussion

Fig. 1 shows the PXRD patterns of as-synthesized Y_2O_3. The peaks were found to be in agreement with the JCPDS 41-1105 reference, corresponding to the [222], [400], [411], [332], [431], [440], [611], and [622] planes. It confirms the formation of single-phase cubic crystalline yttrium nanoparticles. The formation of a single phase is attributed to the high in-situ temperature generated during combustion reaction. The crystallites sizes were calculated using Scherer's formula and were found to be in the range of 18–23 nm. Further, the interplanar spacing (d ≈ 3.055 Å), the cell constant (a ≈ 10.583 Å) and the particle density (ρ ≈ 5.059 g cm^{-3}) were also estimated [19,20].

Fig. 2 shows the SEM profile of pureY_2O_3 depicting the spatial structure of the loosely agglomerated particles which are fluffy and crispy with pores and voids. The morphology of the synthesized sample depends on the nature and concentration of organic fuel. During combustion, yttrium nitrate impregnates into the polymeric product and gets ignited. Heat dissipates by the evolution of gaseous products in minimization and thus it leads to localization of the heat due to the polymeric nature of the fuel [21].

Fig. 3 shows the characteristic FT-IR peaks observed at 875 and 566 cm^{-1} and they are attributed to the stretching of Y–O. The peak at 1433 cm^{-1} due to residual nitrate and organic matter in Y_2O_3 and the broad band with peak at ~3395 cm^{-1} is attributed to the stretching mode of O–H from the water crystallization in the complex [18,22,23].

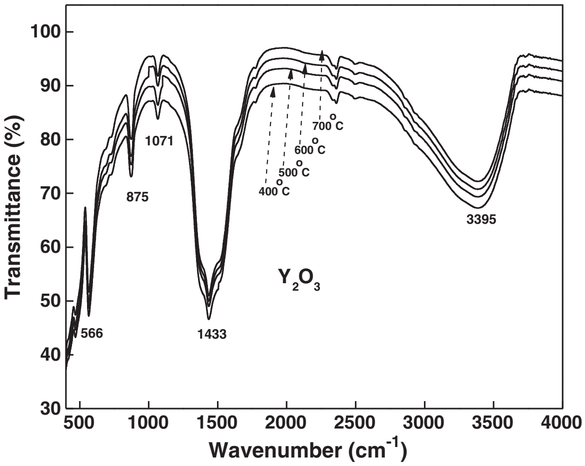

Fig. 3. FTIR spectrum of combustion synthesized Y_2O_3.

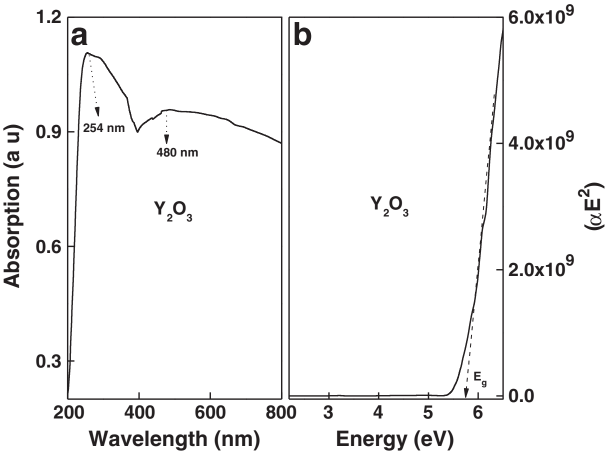

Fig. 4. (a) Optical absorption of combustion synthesized Y_2O_3 and (b) variation of $(\alpha E)^2$ with photon energy.

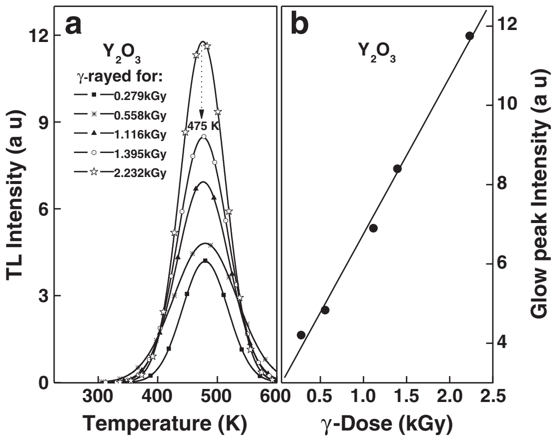

Fig. 6. (a) TL glow curves of combustion synthesized Y_2O_3 for different γ-ray doses and (b) variation of glow peak intensity with dose.

Fig. 4(a) shows the optical absorption of Y_2O_3 recorded in the range of 190–800 nm.

The absorption spectrum reveals a peak at around 254 nm and a broad absorption with peak at around 480 nm. Tomiki et al. also reported two absorption bands in single crystals of Y_2O_3 in the wavelength region 3.5 to 6.0 eV. The most commonly used method to estimate the energy gap (E_g) is the Tauc relation i.e., $(\alpha E) = K\ (E - E_g)^{1/n}$, where 'E' is the photon energy, 'α' is the optical absorption coefficient, 'K' is constant and 'n' is dependent on the optical transition with an assigned value of 2 and 1/2 for direct allowed and indirect allowed transitions respectively. Fig. 4(b) was obtained by plotting $(\alpha E)^2$ versus 'E' in the high absorption range. For direct allowed transition, energy gap E_g was found to be 5.72 eV by extrapolating the linear region of the plot to $(\alpha\ E)^2 = 0$, if $\alpha \neq 0$. This indicates that the allowed direct transition is responsible for the inter band transition in Y_2O_3 [24].

Fig. 5(a) shows the TL glow curves of Y_2O_3 γ-irradiated for a dose of 2.232 kGy. Earlier, it was calcinated at 400, 500, 600 and 700 °C for 2 h and its effect on thermoluminescence behavior was studied. It was found that the TL glow peak intensity for a particular TL glow peak slightly increases, while its glow peak temperature was not perturbed much. This glow curve was deconvoluted using Origin software and the results are shown in Fig. 5(b). The two prominent TL glows with peaks at 475 and 626 K are well resolved as can be seen from the figure. Fig. 6(a) shows the deconvoluted, low temperature TL glow curves of Y_2O_3, γ-irradiated for doses in the range of 0.279–2.232 kGy, in the temperature range of 350–650 K. These well resolved glows with peak at 475 K are recorded at a heating rate of 5 °C s^{-1}. The TL intensity at the glow peaks are plotted as a function of dose and it is shown in Fig. 6(b). It is observed that a linear relation exist between TL glow peak intensity and γ-dose. This behavior of the sample is useful for dosimetric application. Further, the results indicate that the creations of trapping centers increase with an increase of γ-ray. Each of the above TL glow curves are analyzed based on glow curve shape method modified by Chen [25]. A typical result for a glow curve γ-rayed for 2.232 kGy is shown in Fig. 7. The order of kinetics of glow curves are calculated by measuring the symmetry (geometrical) factor $\mu_g \sim 0.505$ ($\mu_g = \delta/\omega$). The values of τ, δ and ω as indicated in Fig. 7 are calculated. Here, 'τ' is the low-temperature half width of the glow curve i.e. $\tau = T_m - T_1$, 'δ' is the high-temperature half width of the glow curve i.e. $\delta = T_2 - T_m$ and 'ω' is the full width of the glow peak at its half height i.e. $\omega = T_2 - T_1$. From the values of the geometrical factor it is clear that the two glow peaks obey the general order kinetics. The trap depth also known as the activation energy of the luminescence centers is calculated using Chen's equation [26].

$$E_\alpha = C_\alpha\left(\frac{k_B T_m^2}{\alpha}\right) - b_\alpha(2k_B T_m),$$

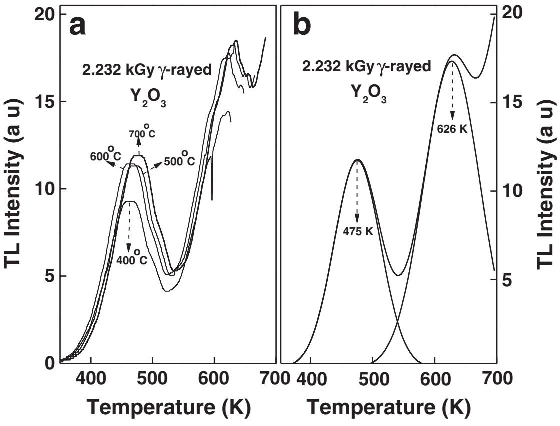

Fig. 5. (a) Thermoluminescence glow curves of combustion synthesized Y_2O_3 and (b) deconvoluted TL glow curve for the dose of 2.232 kGy.

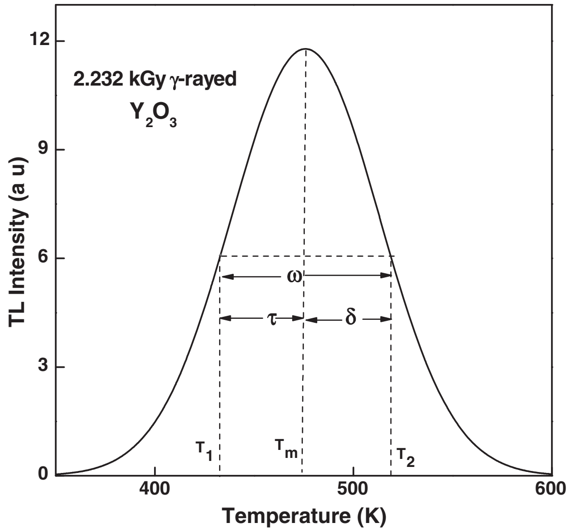

Fig. 7. Representative diagram of different parameters used in the glow-curve shape method.

where 'k_B' is Boltzmann constant, and 'T_m' is peak temperature. The constants 'C_α' and 'b_α' were also calculated by the Chen's equation. The mean activation energy was found to be ~0.679 and ~0.977 eV for 475 and 626 K glow peaks respectively.

4. Conclusions

Y_2O_3 nanoparticles have been synthesized by the EDTA-Na_2 assist combustion technique at low temperature and in a very short time. PXRD pattern of this sample confirms the cubic phase. The crystallites size and the particle density were found to be 18–23 nm and ~5.059 g cm^{-3} respectively. The SEM picture of Y_2O_3 indicated the spatial structure of the loosely agglomerated particles which were fluffy and crispy with pores and voids. The energy gap of Y_2O_3 synthesized in the present work was found to be ~5.72 eV. TL glow curves were analyzed and the trap depths for the two luminescence centers corresponding to 475 K and 626 K glow peaks were calculated. Further, the γ-irradiated Y_2O_3 shows good TL response, up to the dose of 2.232 kGy. It implies that the phosphor synthesized in the present work finds potential use in radiation dosimetry.

Acknowledgments

One of the authors, J.R. Jayaramaiah is thankful to "ISRO-ISEC, advanced devices and radiation cell, Bangalore" for providing facilities for γ-irradiation.

References

[1] Yan Zhu, Yingxue Zhou, Applied Physics A: Materials Science & Processing 92 (2008) 275–278.
[2] A. Konard, T. Fries, A. Gahn, F. Kummer, U. Herr, R. Tidecks, K. Samwer, Journal of Applied Physics 86 (1999) 3129–3133.
[3] Tran Kim Anh, Nguyen Vu, Pham Thi, Minh Chau, Advances in Natural Sciences 182 (2006) 63–69.
[4] J.A. Capobianco, F. Vetron, T. D'Alesio, Physical Chemistry Chemical Physics 2 (2000) 3203–3207.
[5] Zhang Junying, Zhang Zhongtai, Tang Zilong, Lin Yuanhua, Zheng Zishan, Journal of Materials Processing Technology 121 (2002) 265–268.
[6] Gun Young Hong, Byung Soo Jeon, Young Kil Yoo, Journal of the Electrochemical Society 148 (2001) 161–166.
[7] Y.P. Fu, S. Tsao, C.T. Hu, Journal of Alloys and Compounds 395 (2005) 227–230.
[8] Y.P. Fu, S. Tsao, C.T. Hu, Y.D. Yao, Journal of Alloys and Compounds 395 (2005) 272–276.
[9] J.G. Huang, H.R. Zhuang, W.L. Li, Materials Research Bulletin 38 (2003) 149–159.
[10] Xia Li, Hong Liu, Jiyang Wang, Xudong Zhang, Hongmei Cui, Optical Materials 25 (2004) 407–412.
[11] Y.C. Kang, Y.S. Chung, S.B. Park, Journal of the American Ceramic Society 82 (1999) 2056–2060.
[12] Zhai Yongging, Yao Zihua, Ding Shiwen, Qiu Mande, Zhai Jian, Materials Letters 57 (2003) 2901–2906.
[13] S. Erdei, R. Roy, G. Harshe, H. Juwhari, D. Agarwal, F.W. Ainger, W.B. White, Materials Research Bulletin 30 (1995) 745–753.
[14] X.J. Wang, L.D. Zhang, J.P. Zhang, G. He, M. Liu, L.Q. Zhu, Materials Letters 62 (2008) 4235–4237.
[15] Hergen Eilers, Brain M. Tissue, Chemical Physics Letters 251 (1996) 74–78.
[16] M. Kottaisamy, D. Jeyakumar, R. Jagannathan, M. Mohan Rao, Materials Research Bulletin 31 (1996) 1013–1020.
[17] Bipin Bihari, Hergen Eilers, Brian M. Tissue, Journal of Luminescence 75 (1997) 1–10.
[18] Tao Ye, Zhao Guiwen, Zhang Weiping, Xia Shangda, Materials Research Bulletin 32 (1997) 501–506.
[19] H.P. Klug, L.E. Alexander, X-ray Diffraction Procedures, 2nd ed. John wily and sons, New York, 1974.
[20] Fu. Yen-pei, Shaw-Bing Wen, Chin-shang Hsu, Journal of Alloys and Compounds 458 (2008) 318–322.
[21] Jungsik Bang, Mostafa Abboudi, Billie Abrams, Paul H. Holloway, Journal of Luminescence 106 (2004) 177–185.
[22] Pramod K. Sharma, R. Nass, H. Schmidt, Optical Materials 10 (1998) 161–169.
[23] Juan Wang, Xu. Yunhua, Mirabbos Hojamberdiev, Journal of Non-Crystalline Solids 355 (2009) 903–907.
[24] Numan Salah, Sami S. Habib, Zishan H. Khan, Salim Al-Hamedi, S.P. Lochab, Journal of Luminescence 129 (2009) 192–196.
[25] Junying Zhang, Zhongtai Zhang, Zilong Tang, Yuanhua Lin, Journal of Applied Physics 40 (1969) 570–585.
[26] R. Chen, Y. Kirsh, Analysis of Thermally Stimulated Process, Pergamon press, Oxford, 1981, p. 159.